Separation Science and Technology
Publication details, including instructions for authors and subscription information:
http://www.informaworld.com/smpp/title~content=t713708471

Kinetic and equilibrium study of the separation of three chiral center drug, nadolol, by HPLC on a novel perphenyl carbamoylated β-cyclodextrin bonded chiral stationary phase

Xin Wang[a]; Chi Bun Ching[a]
[a] Department of Chemical Engineering, National University of Singapore, Singapore, Singapore

Online publication date: 07 October 2002

SEPARATION SCIENCE AND TECHNOLOGY, 37(11), 2567–2586 (2002)

KINETIC AND EQUILIBRIUM STUDY OF THE SEPARATION OF THREE CHIRAL CENTER DRUG, NADOLOL, BY HPLC ON A NOVEL PERPHENYL CARBAMOYLATED β-CYCLODEXTRIN BONDED CHIRAL STATIONARY PHASE

Xin Wang* **and Chi Bun Ching**

Department of Chemical Engineering, National University of Singapore, 10 Kent Ridge Crescent, Singapore 119260, Singapore

ABSTRACT

A column packed with novel perphenyl carbamoylated β-cyclodextrin (β-CD) immobilized onto silica gel was used to separate nadolol by high performance liquid chromatography. Resolution of three of the four stereoisomers of nadolol was obtained by the complete separation of the most active enantiomer (*RSR*)-nadolol in reversed phase. The optimum separation condition for the mobile phase contained 80% buffer solution (1% TEAA, pH 5.5) and 20% methanol. The bed voidage, axial dispersion coefficient, overall mass transfer coefficients as well as equilibrium constants for the chromatographic enantiomeric separation were evaluated by moment analysis on the basis of solid film linear driving force model. The equilibrium constants

*Corresponding author. Fax: 65-8731994; E-mail: engp9191@nus.edu.sg

were found to be 2.94, 3.46, and 5.45 for the (*SRS*)- and (*SSR*)-nadolol, (*RRS*)-nadolol, and (*RSR*)-nadolol, respectively. Their overall mass transfer coefficients were found to be 669.3, 846.3, and 106.4 min^{-1}, respectively. The simulated results matched the experimental profiles quite well, which confirmed the validity of model parameters obtained in this study.

Key Words: Enantioseparation; Nadolol; Kinetic; Equilibrium; High performance liquid chromatography; Three chiral center; β-Cyclodextrin chiral stationary phase

INTRODUCTION

The chirality of drugs is an important issue from the pharmacological, pharmacokinetic, toxicological, and regulatory points of view (1–5). Owing to the strict regulation by governments and pressure from the public and academic organizations, there is a need to develop optically pure drugs (6). Recently, high performance liquid chromatography (HPLC) using chiral stationary phases (CSPs) has received increasing attention as a preparative-scale enantioseparation method (7–9).

Nadolol, 5-{3-[(1,1-dimethylethyl)amino]-2-hydroxypropoxy}-1,2,3,4-tetrahydro-*cis*-2,3-naphthalenediol, is a β-blocker drug widely used in the management of hypertension and angina pectoris. Its chemical structure has three stereogenic centers, which allow eight possible stereoisomers. However, the two hydroxyl substituents on the cyclohexane ring are fixed in the cis configuration which precludes four stereoisomers. Currently, nadolol is marketed as an equal mixture of its four stereoisomers, designated as the diastereomer mixtures of "racemate A" and "racemate B," as shown in Fig. 1. Racemate A is a mixture of the most active stereoisomer I [(*RSR*)-nadolol] and its enantiomer II [(*SRS*)-nadolol] in 1:1 molar ratio, whereas racemate B is a mixture of stereoisomer III [(*RRS*)-nadolol] and its enantiomer IV [(*SSR*)-nadolol] is also in 1:1 molar ratio. For a safer and more effective use, it is better to separate the enantiomer (*RSR*)-nadolol before use.

Several chiral HPLC methods have been used for the separation of the individual stereoisomers of nadolol on different stationary phases. Pirkle urea-type CSP of (*S*)-indoline-2-carboxylic acid and (*R*)-1-(α-naphthyl)ethylamine (Chirex 3022) was employed by Aboul-Enein and Al Duraibi (10) under normal phase mode and three partially resolved peaks were obtained for nadolol. Lee et al. (11) investigated the separation of nadolol also in normal phase and failed to resolve more than three peaks while using Chiralcel-type or Pirkle-type CSP. Armstrong et al. (12) partially resolved nadolol by using a native cyclodextrin bonded column. The separation was achieved by using mobile phases constituting of a mixture of polar organic solvents, and the separation was not

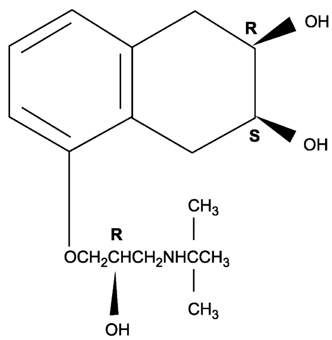

I (RSR-nadolol)

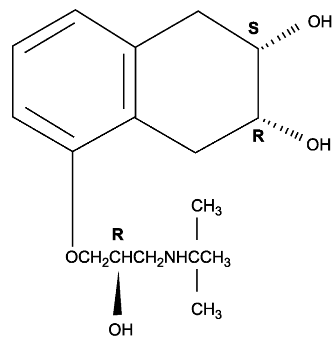

III (RRS-nadolol)

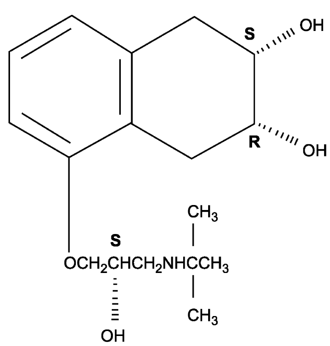

II (SRS-nadolol)

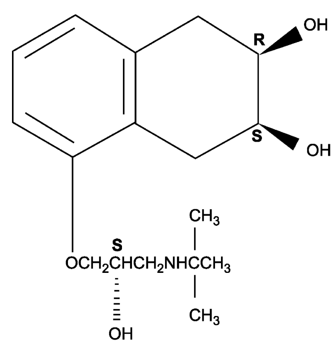

IV (SSR-nadolol)

Figure 1. Chemical structures of stereoisomers of nadolol.

obtained in the reversed-phase mode where inclusion complexation is prevalent. The full resolution of all four optical isomers was achieved by using α1-acid glycoprotein (AGP) stationary phase (11). However, the AGP column, like all protein-based CSPs, has a very low capacity and is easily overloaded. This makes the preparative separations difficult or impossible. In addition, the overall stability of this CSP is still less than desired.

Cyclodextrin (CD)-based stationary phases have been used successfully for the enantiomeric separation of a wide variety of drugs (13) and other optical isomers (14) because of its well-known characteristic property of being able to form inclusion complexes (15). The unique property of cyclodextrin is its "bifunctional" nature arising from its structure, i.e., the cavity is relatively hydrophobic while the external faces are hydrophilic (15). These two properties together with the chirality of cyclodextrin (each glucose unit is chiral) contributed to its chiral recognition abilities (16,17). Recently, a novel perphenyl carbamoylated β-CD covalently bonded CSP was developed by our group (18). A Singapore patent and a U.S. patent have been filed (19,20). The new procedure afforded structurally well-defined CSPs and easily controlled batch-to-batch reproducibility. This stationary phase has good stability and can be used with the wide range of HPLC solvents. It also demonstrates good enantioseparation of drugs in the reversed phase where the traditional β-CD CSP encounters difficulties. The reversed-phase separation replaces highly flammable and toxic hexane with buffer solution for much safer operation in laboratory and possible industry applications. To the best of our knowledge, until now almost all the efforts of enantioseparation of nadolol were performed at analytical scale which did not show much interests in the preparative or productive separation of the active enantiomer of nadolol. Furthermore, most of the separation conditions consist of either normal phase or polar organic phase, which were more expensive and dangerous compared with the reversed phase.

To achieve preparative separation of nadolol by chromatographic method, the kinetic and equilibrium of enantioseparation of nadolol on the columns packed by this novel CSP are important. In this study, resolution of three of the four stereoisomers of nadolol was achieved with a complete separation of the most active stereoisomer (*RSR*)-nadolol on a column, which was packed with perphenyl carbamoylated β-CD immobilized onto silica gel. The column was characterized by the bed voidage and the axial dispersion coefficient. The linear driving force model was used to describe and model the adsorption process. The moment analysis and the parameters obtained, which include the kinetics of mass transfer and equilibrium constant, were used for the simulation of band profiles.

THEORETICAL SECTION

The Rate Models for Chromatography

The differential mass balance equation for a component i over a slice of the column is written as (21)

$$\frac{\partial C_i}{\partial t} + F\frac{\partial C_{S,i}}{\partial t} + v\frac{\partial C_i}{\partial z} = D_L\frac{\partial^2 C_i}{\partial z^2} \tag{1}$$

where C_i and $C_{S,i}$ are the concentrations of component i in mobile phase and stationary phase, respectively, F the phase ratio and equals to $(1-\varepsilon)/\varepsilon$, where ε is the bed voidage of the column, v the interstitial velocity, D_L the axial dispersion coefficient, and z and t the space and time coordinates. Assumptions made in the derivation of the above equation include: homogeneous packing, negligibility of the compressibility of mobile phase, and thus constant mobile phase velocity along the column, constant axial dispersion coefficient along the column, isothermal bed, and radial homogeneous of the column.

In the solid film linear driving force model, the mass transfer resistance is believed to be located in the thin solid film in which the stationary phase concentration varies from the equilibrium concentration q_i^* at the contacting surface to the stationary phase average concentration $C_{S,i}$. As the mass transfer rate is believed to be proportional to the concentration difference, the rate equation is written as:

$$\frac{\partial C_{S,i}}{\partial t} = k_i(q_i^* - C_{S,i}) \tag{2}$$

In the diluted region, linear isotherm was used:

$$q_i^* = K_i C_i \tag{3}$$

Moment Analysis

The well-proved method of moment analysis was used to determine the hydrodynamics of the column (22,23). The nth moment of the band profile at the exit of a chromatographic column of length $z = L$ is defined as:

$$M_n = \int_0^\infty C(t, z = L) t^n \, dt \tag{4}$$

Due to greater physical significances, the first moment is normally defined as normalized moment and moments higher than the first are defined as central moments, which are measured relative to the first moment:

$$\mu_1 = \frac{\int_0^\infty C(t, L) t \, dt}{\int_0^\infty C(t, L) dt} \tag{5}$$

$$\overline{\mu_2} = \sigma^2 = \frac{\int_0^\infty C(t, L)(t - \mu_1)^2 \, dt}{\int_0^\infty C(t, L) dt} \tag{6}$$

By definition, the zero moment of the concentration profile of an eluted peak is simply the area of the peak. The first moment is the center of gravity of the concentration profile. In chromatography, it relates to peak retention time and therefore to the strength of adsorption. It will coincide with the peak maximum only when the peak is symmetrical. The second moment is peak variance, which is chromatographically related to peak spreading, caused by departures from linear adsorption isotherms and by mass transfer resistances. It is obvious to notice that $\sigma^2 = \mu_2 - \mu_1^2$.

For the solid film linear driving force model, the corresponding expression for the first and second moment is (23):

$$\mu_1 = \frac{L}{v}\left[1 + \left(\frac{1-\varepsilon}{\varepsilon}\right)K\right] \tag{7}$$

$$\overline{\mu_2} = \frac{2L}{v}\left\{\frac{D_L}{v^2}\left[1 + \left(\frac{1-\varepsilon}{\varepsilon}\right)K\right]^2 + \left(\frac{1-\varepsilon}{\varepsilon}\right)\frac{K}{k}\right\} \tag{8}$$

Also the height equivalent to a theoretical plate (HETP) is defined as:

$$\text{HETP} = \frac{L}{N} \tag{9}$$

The expression for HETP was derived from the moment analysis of the solution of the general rate model in the Laplace domain (23):

$$\text{HETP} = \frac{L}{N} = \frac{\sigma^2 L}{\mu_1^2} = \frac{2D_L}{v} + 2v\left(\frac{\varepsilon}{1-\varepsilon}\right)\frac{1}{kK}\left(1 + \frac{\varepsilon}{(1-\varepsilon)K}\right)^{-2} \tag{10}$$

Equation (10) contains two separate parameters of interests, the axial dispersion coefficient and the overall mass transfer coefficient. It is evident from the equation that the contributions of axial dispersion and the various mass transfer resistances are linearly additive.

Model Parameters

Bed Voidage

Three different types of column porosity, which are total porosity ε_T, external bed porosity ε_{ext} (or bed voidage ε), and the internal porosity ε_i, are related by the equation:

$$\varepsilon_T = \varepsilon_{ext} + (1 - \varepsilon_{ext})\varepsilon_{int} \tag{11}$$

The bed voidage can be evaluated from the zero retention time of a nonadsorbed component to the stationary phase. For a component that enters the pore system, but does not adsorb on the surface of the stationary phase, the retention time of such a component is given by

$$t_{0R} = \frac{V\varepsilon_T}{\dot{V}} = \frac{L\varepsilon_T}{u} \tag{12}$$

where u and $\dot{V}$ are the superficial velocity and volumetric flow rate of the mobile phase, respectively. According to Eq. (11), if the internal particle porosity is known, the bed voidage ε which is used for defining phase ratio in this study, can be calculated from the total porosity of the column.

Axial Dispersion Coefficient

When a fluid flows through a packed bed, there is a tendency for axial mixing to occur which reduces the efficiency of separation. All the phenomena contributed to axial mixing, except that of mass transfer resistance, are lumped into an axial dispersion coefficient. Two main mechanisms contributed to axial dispersion are molecular diffusion and eddy diffusion. In a packed bed, it is impossible for the mobile phase to move very far along a straight line without hitting the surface of a particle. The channels follow tortuous paths around the particles. As a first approximation, molecular diffusion and eddy diffusion are additive, and the axial dispersion coefficient D_L, is given by

$$D_L = \gamma_1 D_m + \gamma_2 d_P v \tag{13}$$

where d_P is the particle diameter and γ_1 and γ_2 the geometrical constants (23). For enantioseparation of chiral substances whose physical properties (including diffusion coefficients D_m) are identical, their axial dispersion coefficients D_L are equal.

D_L can also be expressed as $D_L = \eta D_m + \lambda v$ for convenience, where η is the tortuosity factor for a packed column and λ the flow-geometry dependent constant. As the molecular diffusivity D_m of liquid is too small to contribute significantly to axial dispersion even at low Reynolds numbers, Eq. (13) can be simplified as

$$D_L = \lambda v \tag{14}$$

Kinetic Data

The overall mass transfer coefficient, k, is composed of two separate mass transfer mechanisms—the external and internal resistances to mass transfer

$$\frac{1}{kK} = \frac{d_P}{3k_f} + \frac{d_P^2}{15KD_e} \tag{15}$$

where k_f is the external film mass transfer coefficient and D_e the effective diffusion coefficient. Wilson and Geankoplis (24) proposed the following correction to describe the dependence of k_f on velocity at low Reynolds numbers in a liquid system:

$$k_{\mathrm{f}} = 1.09v[Re\,Sc]^{-2/3} \tag{16}$$

It is clear that k will be independent of liquid velocity provided that the influence of external film resistance is negligible. Under the experimental conditions in this work, $d_{\mathrm{P}}/3k_{\mathrm{f}} \ll d_{\mathrm{P}}^2/15KD_{\mathrm{e}}$ because k_{f} estimated from Eq. (16) is greater than D_{e} by at least a few orders of magnitude (also K is small). Ching and Chu (25) investigated a chromatographic system similar to this study. One may then neglect the contribution of external film mass transfer resistance, thus simplifying Eq. (15) to

$$\frac{1}{kK} = \frac{d_{\mathrm{P}}^2}{15KD_{\mathrm{e}}} \tag{17}$$

which states that k can be regarded as a constant under the experimental conditions employed in this work.

MATERIALS, INSTRUMENTATION, AND EXPERIMENTAL PROCEDURE

Synthesis of the CSP

The CSP was prepared with a pre-derived procedure. Perfunctionalized cyclodextrins were first synthesized, purified, and characterized and then chemically anchored on the surface of aminized silica gel via the hydrolytically stable urethane linkage. The detailed synthesis procedures were described elsewhere (18). The silica gel was supplied by Hypersil (UK) with a particle size of 15 μm. Empty column (250 mm × 4.6 mm) assembly was purchased from Phenomenex (USA). The column was packed using an Alltech pneumatic HPLC pump (Alltech, USA).

Materials and Apparatus

The HPLC-grade methanol was obtained from Fisher Scientific (Leics, UK). Glacial acetic acid and triethylamine were obtained from Merck (Germany). The HPLC water was made in the laboratory using a Millipore ultra-pure water system. 1,3,5-Tri-*tert*-butyl benzene (TTBB) was purchased from Aldrich (USA). The racemate mixture of nadolol was purchased from Sigma (St. Louis, MO). The four stereoisomers of nadolol (SQ12148, SQ12149, SQ12150, and SQ12151), all lot #2, were kindly provided by the research chemical distribution center of Bristol-Myers Squibb Company (Princeton, NJ). SQ12148, SQ12149, SQ12150, and SQ12151 represent (*RSR*)-, (*RRS*)-, (*SRS*)-, and (*SSR*)-nadolol, respectively. All purchased products were used without further purification.

The experiments were carried out with a Shimadzu LC-10ATVP chromatographic system (Kyoto, Japan). The system consists of two LC-$10AT_{vp}$ pumps (A and B), an online degasser DGU-14A, an SIL-$I0AD_{vp}$ auto-injector, and an SPD-$10A_{vp}$ UV–Vis detector. The software CLASS-VP 5.032 was used to control the system and record the detector signal.

Experimental Procedure

The experiments were conducted at room temperature of about 24°C. All experiments were carried out in the reversed-phase mode. The mobile phase used was a binary mixture of solvent A and solvent B. Solvent A contained pure methanol and solvent B contained buffer solution of triethylamine (TEA) adjusted with acetic acid to the desired pH value. Solvents A and B were delivered by pumps A and B, respectively, and were mixed thoroughly in a low dead volume mixer after the pumps. The enantioseparation can be affected by methanol concentration, TEAA concentration, and the pH value of the mobile phase. All these parameters were changed systematically in order to optimize the separation condition. The optimum mobile phase was found in previous studies to contain 80% buffer solution (1% TEAA, pH 5.5) and 20% methanol. The resolution of the first and second peaks was defined as critical peaks, which were used to evaluate the separation results. TTBB was dissolved in methanol at a concentration of 0.128 mg/mL. Racemate of nadolol was dissolved in the mobile phase at a concentration of 0.068 mg/mL. All samples were first degassed in a model LC 60H ultrasonic bath before 20 μL of which were injected into the column by the auto-injector. Signals were detected with the UV detector with wavelength set at 220 and 280 nm for TTBB and nadolol, respectively. The dead time of the column was determined by injecting pure TTBB at 220 nm.

For a given chromatographic system (sample-mobile phase-column), several response peaks were measured at different flow rates of the mobile phase. These peaks gave the necessary information on the determination of the adsorption equilibrium and kinetic coefficients.

RESULTS AND DISCUSSION

Elution Order of the Enantiomers of Nadolol

In order to determine the elution order of enantiomers of nadolol, samples of the four stereoisomers, namely (*SRS*)-, (*SSR*)-, (*RRS*)-, and

(*RSR*)-nadolol, were injected into the column, respectively, under the same chromatographic conditions as that for the racemic mixture of nadolol. It was found that one member of each enantiomeric pair [(*SRS*)-nadolol and (*SSR*)-nadolol] had nearly the same retention time, e.g., they had retention times of 23.8 and 24.0 min, respectively, at a flow rate of 0.3 mL/min. Despite the small difference between the retention time of these two components, they could not be separated when racemate nadolol was injected. They eluted together and overlapped in the first peak of the elution chromatogram due to the bandwidth effect, which were results of mass transfer resistance and axial dispersion in the column. The first peak had twice the area of the second and third peak of (*RRS*)-nadolol and (*RSR*)-nadolol, respectively. The two stereoisomers of (*SRS*)-nadolol and (*SSR*)-nadolol were considered as one component in this study and thus they had the same equilibrium constant and mass transfer coefficients.

Determination of Bed Voidage

1,3,5-Tri-*tert*-butyl benzene has been widely used for the determination of column dead time t_{0R} for various CSPs (9). The structure of TTBB is shown in Fig. 2.

Although the sorption to the perphenyl carbamoylated β-cyclodextrin is strongly supported by a phenyl group, this group is surrounded and shielded by the three *tert*-butyl groups in the case of TTBB. Furthermore, an exclusion mechanism is not likely to occur due to the relatively small molecular size of TTBB. Therefore, TTBB is not retained in the stationary phase and was chosen to determine the total porosity ε_T of the column in this study.

The total porosity, ε_T, was determined from the response to a pulse injection of TTBB. The retention time of TTBB in the column was corrected by

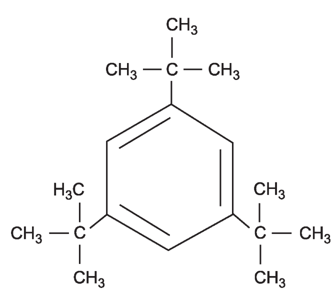

Figure 2. Molecular structure of TTBB.

deducting the retention time of TTBB peak measured when the injector directly connected to the detector.

For the nonadsorbed component of TTBB that can enter the pores of the stationary phase particles, the zero retention time was given by Eq. (12). From the plot of mean retention time against the inverse flow rate in Fig. 3, the total porosity ε_T was found to be 0.77.

The following correlation was used in this study to evaluate the bed voidage of the column, which was suggested by Suzuki (22), Ruthven (23) and Wakao and Smith (26):

$$\varepsilon_T = 0.45 + 0.55\varepsilon \tag{18}$$

The bed voidage was found to be 0.58 for the column.

Determination of Axial Dispersion

Combining Eqs. (10) and (14) and rearranging,

$$\mathrm{HETP} = 2\lambda + 2v\left(\frac{\varepsilon}{1-\varepsilon}\right)\frac{1}{kK}\left(1 + \frac{\varepsilon}{(1-\varepsilon)K}\right)^{-2} \tag{19}$$

In this study, the axial dispersion coefficient in the column was evaluated from HETP of the nonadsorbed TTBB peaks. The TTBB compound penetrates the sorbent rapidly and thus has negligible influence of inter-phase mass transfer on dispersion. This means that the mass transfer coefficient k has a higher order of

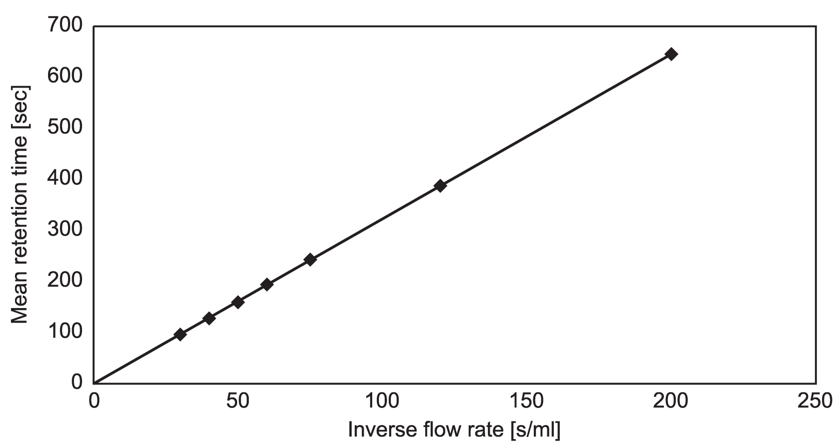

Figure 3. Plot of mean retention time of TTBB vs. inverse of mobile phase flow rate.

magnitude and thus the mass transfer resistance can be neglected and it hardly contributes to the broadening of the peak. It is also known that TTBB is not adsorbed in the CSP ($K = 0$). In both cases, the second term of Eq. (19) is equal to zero. Under such condition of axial dispersion control, one would expect to find a constant HETP, independent of liquid velocity, as shown in the following equation:

$$\mathrm{HETP} = \frac{2D_L}{v} = 2\lambda \tag{20}$$

In our experiment, it was found that TTBB rarely dissolved in the mobile phase [buffer solution of 1% TEAA (pH 5.5)/methanol = 80/20]. However, TTBB was easily dissolved in methanol. Since axial mixing in the chiral column is determined by the flow pattern rather than by molecular diffusion, axial dispersion coefficient determined by using methanol as mobile phase should have the same value as that obtained in the real mobile phase.

When using Eq. (10) to calculate HETP, it was found that the calculation of the second moment was prone to error, because slight detector signal baseline shift or even the different choices of peak start and end positions can lead to large variations. In this study, an alternative method was used to calculate HETP from the column theoretical numbers based on Eq. (10).

For symmetric peaks, the theoretical numbers of the column is given as

$$N = 5.54\left(\frac{t_R}{W_{0.5}}\right)^2 \tag{21}$$

For asymmetric peaks, the exponential-modified Gaussian equation (EMG) (27) was used:

$$N = 41.7\frac{\left(\frac{t_R}{W_{0.1}}\right)^2}{\frac{b_{0.1}}{a_{0.1}} + 1.25} \tag{22}$$

The plot of HETP of TTBB vs. the interstitial velocity of mobile phase given in Fig. 4 shows a straight line with very little variation to the flow rate. The D_L could be determined from the HETP corresponding to $v = 0$ which gives

$$D_L = 0.00275v\,(\mathrm{cm})$$

Determination of Equilibrium Data

In deviation of Eq. (7) in the moment analysis, it was assumed that the isotherm was linear. To fulfill this requirement, all pulse experiments need to be

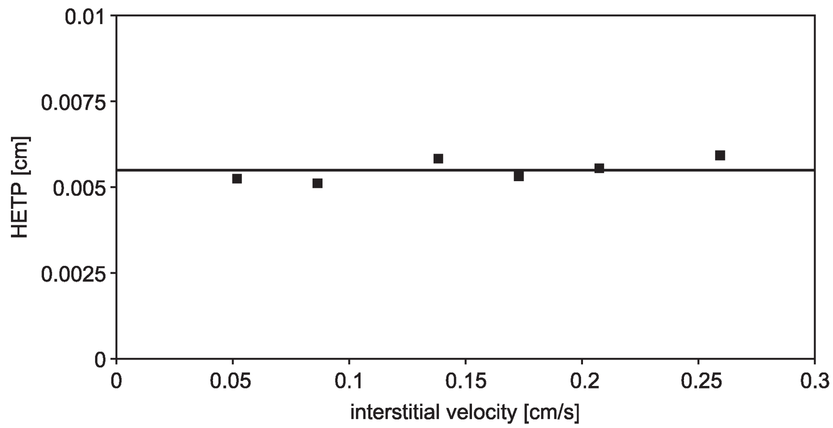

Figure 4. Plot of HETP of TTBB vs. interstitial velocity of mobile phase on the column.

carried out under linear conditions. Therefore, dilute nadolol samples were used in the chromatographic experiment and with 10-fold variation in the amount of samples injected, there were no difference for the first moments of the three peaks. According to the experimental results, the concentration of nadolol solution at 0.068 mg/mL is believed to be in the linear isotherm region.

The first moments of the three components of nadolol were plotted against the inverse superficial velocity of mobile phase in Fig. 5. Straight lines were fitted

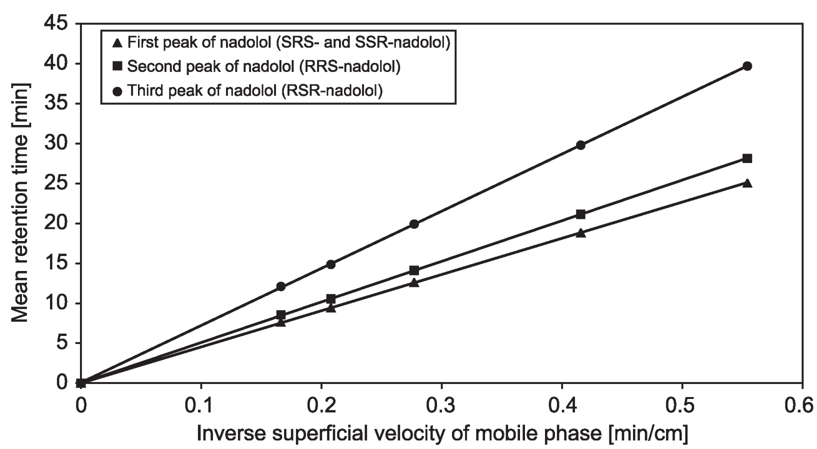

Figure 5. Plot of first moments of three components of nadolol vs. inverse superficial velocity of mobile phase on the column.

to the experimental points. As the retention times should become zero if the interstitial velocity is infinite, the lines were forced through the origin. All fitted lines were in good agreement with the experimental points. According to Eq. (7), the equilibrium constants were determined from the slopes of the lines, which were found to be 2.94, 3.46, and 5.45 for the stereoisomers (*SRS*)- and (*SSR*)-nadolol (considered as one component), (*RRS*)-nadolol, and (*RSR*)-nadolol, respectively.

Determination of Mass Transfer Coefficient of the Chiral Column

According to Eq. (19), a plot of HETP against interstitial velocity of mobile phase for the three components of nadolol should give HETP which increases approximately linearly with velocity, as shown in Fig. 6. The overall mass transfer coefficient k can be determined from the slopes and were found to be 669.3, 846.3, and 106.4 min^{-1} for components (*SRS*)- and (*SSR*)-nadolol, (*RRS*)-nadolol, and (*RSR*)-nadolol, respectively. These components correspond to the first, second, and third peaks, respectively, in Fig. 7. The results show that the mass transfer coefficients of the first two components are 6.29 and 7.95 times larger than that of the third component. Clearly, the most retained component of (*RSR*)-nadolol has the least mass transfer coefficient in the CSP compared with the other two rapidly eluting ones.

Since (*RSR*)-nadolol and (*SRS*)-nadolol are enantiomers, which constitute racemate A (SQ12181), they have identical physical and chemical

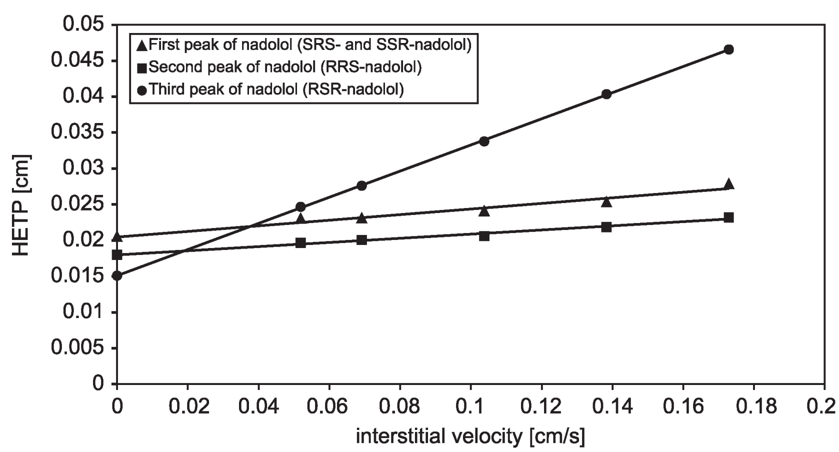

Figure 6. Plot of HETP of enantiomers of nadolol vs. the interstitial velocity on the column.

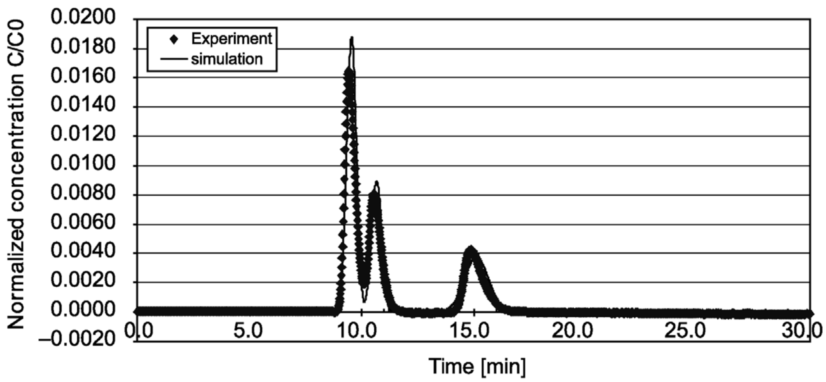

Figure 7. Comparison of the simulated and experimental band profiles of racemate nadolol. Conditions: flow rate $= 0.8$ mL/min, $C_0 = 0.068\,\mathrm{mg/mL}$ (linear region).

properties in an achiral environment. Therefore, the contributions of film diffusion and pore diffusion to the lumped mass transfer coefficient should be equal for both substances. The large difference in the lumped mass transfer coefficient could be due to the different kinetics of adsorption and desorption process. The same postulation could be made for enantiomers (*RRS*)-nadolol and (*SSR*)-nadolol which constitute racemate B (SQ12182). (*SRS*)-nadolol and (*SSR*)-nadolol are diastereomers which have different physical properties. Both the adsorption–desorption rate and the mass transfer rate in the thin solid film and macropore–micropore differ from each other. The same lumped mass transfer coefficient of (*SRS*)-nadolol and (*SSR*)-nadolol could be due to the counterbalance of these two effects. It should also be mentioned that axial mixing in the column is determined by the flow pattern rather than by molecular diffusion. The contribution of axial mixing to HETP should therefore be approximately the same for the four enantiomers of nadolol. Therefore, in Fig. 6, the three lines should give the same intercept at $v = 0$. The slight difference between them could be due to experimental errors.

The CSP in this study were synthesized and packed in a way to achieve high resolution and fast separation of chiral compounds, like most commercially available columns. The effect of mass transfer resistance (including that of external film resistance, intraparticle diffusion resistance, and adsorption/desorption resistance) has only a very modest effect on the response curves for a column having a reasonable high efficiency. Hence, a lumped mass transfer parameter can be used quite effectively even though it fails to investigate the nature of the specific mass transfer resistance.

Simulation Results

Chromatography is a complex phenomenon. In this process, all the factors such as fluid dynamics, mass transfer phenomena, and equilibrium thermodynamics play an important role in the result of separation. The bed voidage ε, axial dispersion coefficient D_L, equilibrium constant K_i, and mass transfer coefficient k_i obtained from experimental results were used to simulate the elution profiles of racemate nadolol.

The corresponding boundary and initial conditions for Eqs. (1) and (2) are given as follows.

Danckwerts boundary conditions:

$$D_L \frac{\partial C_i}{\partial z}(z = 0, t) = -v[C_i(z = 0^-, t) - C_i(z = 0^+, t)] \tag{23}$$

$$\frac{\partial C_i}{\partial z}(z = L, t) = 0 \tag{24}$$

Initial conditions:

$$C_i(z, t = 0) = C_{S,i}(z, t = 0) = 0 \tag{25}$$

$i = 1, 2, 3$ corresponds to the first, second, and third components of nadolol, respectively.

The feed to the column was represented by a square pulse:

$$\begin{cases} C_1(z = 0^-, t)/C_0 = 0.5, \\ C_2(z = 0^-, t)/C_0 = 0.25, \qquad \text{when } 0 \le t \le t_{\text{inj}} \\ C_3(z = 0^-, t)/C_0 = 0.25, \end{cases} \tag{26}$$

$$C_1 = C_2 = C_3 = 0 \quad \text{when } t > t_{\text{inj}} \tag{27}$$

The experiments with diluted feed concentrations of nadolol (in the region of linear isotherm) were carried out at different mobile phase flow rates. Their band profiles were normalized from detector signals (mV) to dimensionless concentration C/C_0. The PDE systems with the initial and boundary conditions as well as the square pulse injection were solved by a commercial software Femlab 2.0.0.162. The simulated results were compared with the experimental results in Figure 7. It was found that the experimental and simulated results matched quite well. The slight discrepancy of peak shapes for the first and second peaks could probably be due to the difficulty in obtaining accurate HETP for these two components when determining the mass transfer coefficients as they were not baseline separated.

CONCLUSION

In this study, chromatographic resolution of three of the four stereoisomers of nadolol was obtained on the novel perphenyl carbamoylated β-CD CSP in reversed phase with a complete separation of the most active enantiomer (*RSR*)-nadolol. The three peaks of nadolol in the chromatogram were identified by injecting the four stereoisomers into the HPLC system under the same chromatographic conditions. Enantiomers (*SRS*)- and (*SSR*)-nadolol, which were considered as one component, eluted together and overlapped in the first elution profiles, while (*RRS*)-nadolol and (*RSR*)-nadolol corresponded to those of the second and third peaks, respectively. The axial dispersion coefficient D_L, equilibrium constant K_i, and overall mass transfer coefficient k_i of the three components of nadolol and the bed voidage ε of the column for the enantioseparation were determined by moment analysis. The axial dispersion coefficient in the column was evaluated to be $0.00275v$ for the three components of nadolol. The equilibrium constants were found to be 2.94, 3.46, and 5.45 for the (*SRS*)- and (*SSR*)-nadolol, (*RRS*)-nadolol, and (*RSR*)-nadolol, respectively. The overall mass transfer coefficients were evaluated to be 669.3, 846.3, and $106.4\,\text{min}^{-1}$ for the three components. The simulated results fit the experimental observations quite well.

Although enantioseparation of all the four stereoisomers of nadolol was not accomplished in the perphenyl carbamated β-CD covalently bonded CSP, three components including that of the most active enantiomer, (*RSR*)-nadolol, were successfully separated. The optimum separation condition and model parameters will be important for the preparative separation of racemate nadolol using a five-zone configuration simulated moving bed (SMB) chromatography. Therefore, this work forms the basis to achieve enantioseparation of these three components of nadolol by five-zone SMB.

NOMENCLATURE

$a_{0.1}$	width of the first half (start to top) of the peak at 10% peak height
C	concentration in mobile phase (mg/mL)
C_S	concentration in stationary phase (mg/mL)
C_0	pulse injection concentration (mg/mL)
D_e	effective diffusion coefficient (cm^2/sec)
D_L	axial dispersion coefficient (cm^2/sec)
D_m	solute molecular diffusivity (cm^2/sec)
d	diameter of the column (cm)
d_P	particle diameter (μm)
F	phase ratio, equal to $(1-\varepsilon)/\varepsilon$
HETP	height equivalent to a theoretical plate (cm)

k	lumped mass transfer coefficient (sec^{-1} or min^{-1})
k_f	external film mass transfer coefficient (cm/min)
K	equilibrium constant (dimensionless)
L	column length (cm)
N	theoretical numbers of the column
q_i^*	equilibrium concentration on stationary phase (mg/mL)
Re	Reynolds number, $v\varepsilon d_P \rho/\mu = v\varepsilon d_P/\gamma$
Sc	Schmidt number, $\mu/\rho D_m$
t_R	mean retention time of an adsorbed component (min)
t_0	mean retention time for an unretained compound (min) (the compound cannot enter the pore system of the stationary phase)
t_{0R}	mean retention time for an unretained compound (min) (the compound can enter the pore system of the stationary phase)
u	superficial velocity (cm/sec)
v	interstitial fluid velocity (cm/sec)
V	column volume (cm^3)
$\dot{V}$	volumetric flow rate of the mobile phase (mL/min)
$W_{0.1}$	width of the peak at the position of 10% peak height
$W_{0.5}$	width of the peak at half peak height
z	space coordinate

Greek Symbols

γ_1	geometrical constants
γ_2	geometrical constants
ε	bed voidage, equal to external bed porosity ε_{ext}
ε_i	internal porosity
ε_T	total porosity
λ	flow-geometry dependent constant in Eq. (14)
μ	dynamic viscosity, $\mu\rho = v$, v is kinetic viscosity
μ_1	the first moment
μ_2	the second central moment
η	tortuosity factor for a packed column
ρ	density of mobile phase

Subscripts

i	component i

ACKNOWLEDGMENTS

The authors thank Bristol-Myers Squibb Company (Princeton, NJ) for kindly providing the four stereoisomers of nadolol in this research work. The financial support of National University of Singapore is gratefully acknowledged.

REFERENCES

1. Rekoske, J.E. Chiral Separations. AIChE J. **2001**, *47* (1), 2–5.
2. Waldeck, B. Biological Significance of the Enantiomeric Purity of Drugs. Chirality **1993**, *5*, 350–355.
3. Testa, B.; Trager, W.F. Racemates Versus Enantiomers in Drug Development: Dogmatism or Pragmatism? Chirality **1990**, *2*, 129–133.
4. Ahuja, S. The Importance of Chiral Separations in Pharmaceuticals. In *Impact of Stereochemistry in Drug Development and Use*; Aboul-Enein, H.Y., Wainer, I.W., Eds.; Wiley: New York, 1997.
5. Abernethy, D.R.; Andrawis, N.S. Stereoisomeric Drugs in the Therapeutics, Clinical Perspectives. In *Drug Stereochemistry, Analytical Methods and Pharmacology*; Wainer, I.W., Ed.; Marcel Dekker: New York, 1993.
6. Stinson, S.C. Chiral Drugs. Chem. Eng. News **1995**, *9*, 44–74.
7. Ruthven, D.M.; Ching, C.B. Counter-Current and Simulated Counter-Current Adsorption. Chem. Eng. Sci. **1989**, *44*, 1011.
8. Ching, C.B.; Lim, B.G.; Lee, E.J.D.; Ng, S.C. Chromatographic Resolution of The Chiral Isomers of Several Beta-Blockers over Cellulose Tris(3,5-Dimethylphenylcarbamate) Chiral Stationary Phase. Chirality **1992**, *4*, 174–177.
9. Ching, C.B.; Lim, B.G. Preparative Resolution of Praziquantel Enantiomers by Simulated Counter-Current Chromatography. J. Chromatogr. **1993**, *634*, 215–219.
10. Aboul-Enein, H.Y.; Al-Duraibi, I.A. Isocratic HPLC Separation of Several Racemic Drugs with Two Stereogenic Centers on a Pirple Urea-Type Chiral Stationary Phase. J. Liq. Chromatogr. Rel. Technol. **1998**, *21* (12), 1817–1831.
11. Lee, C.R.; Porziemsky, J.P.; Aubert, M.C.; Krslovic, A.M. Liquid and High Pressure Carbon Dioxide Chromatography of β-Blockers. J. Chromatogr. **1991**, *539*, 55–69.
12. Armstrong, D.W.; Chen, S.; Chang, C.; Chang, S. A New Approach for the Direct Resolution of Racemic Beta Adrenergic Blocking Agents by HPLC. J. Liq. Chromatogr. **1992**, *15* (3), 545–556.
13. Armstrong, D.W.; Ward, T.J.; Armstrong, R.D.; Beesley, T.E. Separation of Drug Stereoisomers by the Formation of β-Cyclodextrin Inclusion Complexes. Science **1986**, *232*, 1132.
14. Armstrong, D.W.; DeMond, W.; Ala, A.; Hinze, W.; Riehl, T.E.; Bui, K.H. Liquid Chromatographic Separation of Diastereomers and Structural Isomers on Cyclodextrin-Bonded Phases. Anal. Chem. **1985**, *57*, 234.
15. Li, S.; Purdy, W.C. Cyclodextrin and Their Application in Analytical Chemistry. Chem. Rev. **1992**, *92*, 1457–1470.

16. Armstrong, D.W.; Stalcup, A.M.; et al. Derivatized Cyclodextrin for Normal-Phase Liquid Chromatographic Separation of Enantiomers. Anal. Chem. **1990**, *62*, 1610–1615.
17. Ward, T.J.; Armstrong, D.W. Improved Cyclodextrin Chiral Phases: A Comparison and Review. J. Liq. Chromatogr. **1986**, *9*, 40–423.
18. Zhang, L.F.; Wong, Y.C.; Chen, L.; Ching, C.B. A Facile Immobilization Approach for Perfunctionalised Cyclodextrin onto Silica via the Staudinger Reaction. Tetrahedron Lett. **1999**, *40*, 1815–1818.
19. Ng, S.C.; Zhang, L.F; Ching, C.B. U.S. Patent No. 6,017,458.
20. Ng, S.C.; Ching, C.B.; Zhang, L.F. Singapore Patent No. 9,703,0597.
21. Guichon, G.; Golshan-Shirazi, S.; Katti, A. *Fundamentals of Preparative and Nonlinear Chromatography*; Academic Press: Boston, 1994.
22. Suzuki, M. *Adsorption Engineering*; Elsevier: Amsterdam, 1990.
23. Ruthven, D.M. *Principle of Adsorption and Adsorption Processes*; Wiley: New York, 1984.
24. Wilson, E.J.; Geankoplis, C.J. Liquid Mass Transfer at Very Low Reynolds Numbers in Paced Beds. Ind. Eng. Chem. Fundam. **1966**, *5*, 9.
25. Ching, C.B.; Chu, K.H. A Chromatographic Analysis of Hindered Diffusion of Saccharides in Silica Gels. Chromatographia **1989**, *28*, 369.
26. Wakao, N.; Smith, J.M. Diffusion in Catalyst Pellets. Chem. Eng. Sci. **1962**, *17*, 825.
27. Foley, J.P.; Dorsey, J.G. Equations for Calculation of Chromatographic Figures of Merit for Ideal and Skewed Peaks. Anal. Chem. **1983**, *55*, 730–737.

Received October 2001